

NUMERICAL AND EXPERIMENTAL INVESTIGATIONS OF TRANSIENT CAVITATING PIPE FLOW

NUMERIČNE IN EKSPERIMENTALNE RAZISKAVE PREHODNEGA KAVITACIJSKEGA TOKA V CEVI

Anton Bergant[✉], Uroš Karadžić¹

Keywords: pipe flow, transient cavitation, discrete gas cavity model, unsteady skin friction

Abstract

This paper investigates the effects of transient vaporous cavitation caused by the closure of the downstream end ball valve against the discharge. Numerical results are compared with the results of measurements in the simple reservoir-pipeline-valve apparatus. Pressures measured at the end points and at two equidistant positions along the pipeline are compared with computational results as piezometric heads. Comparisons between the results of two distinct water column separation tests and numerical simulations using an advanced discrete gas cavity model show good agreement. Two distinct column separation runs include active and passive column separation cases.

Povzetek

Prispevek obravnava prehodni parni kavitacijski tok induciran z zapiranjem dolvodnega kroglastega zapirala v sistemu pod pretokom. Računski rezultati so primerjani z rezultati meritev v preprosti preizkusni postaji, ki jo sestavljajo rezervoar, cevovod in zapiralo. Tlaki merjeni na dolvodnem in gorvodnem delu cevi in tlaka merjena na ekvidistantnih dolžinah vzdolž cevi so primerjani z izraču-

✉ Corresponding author: Anton Bergant, PhD, Litostroj Power d.o.o., Litostrojska 50, SI-1000 Ljubljana, Slovenia, anton.bergant@litostrojpower.eu

¹Uroš Karadžić, PhD, Univerzitet Crne Gore, Mašinski fakultet, Džordža Vašingtona bb, ME-81000 Podgorica, Montenegro, uros.karadzic@ac.me

nom kot piezometrične višine. Rezultati meritev in izračunov dobljenih s pomočjo naprednega diskretnega plinskega kavitacijskega modela za dva posebna primera pretrganja kapljevinskega stebra se dobro ujemajo. Prvi primer zajema aktivno obliko pretrganja stebra, drugi primer pa predstavlja pasivno obliko pretrganja.

1 INTRODUCTION

Industrial pipeline systems operate over a broad range of operating regimes. Induced unsteady flows in pipes and system components (valve, pump, turbine) are the source of many unwanted loads in industrial installations, including severe pressure pulsations and pipeline vibrations [1], [2]. Water hammer is the propagation of pressure waves along liquid-filled pipelines, and it is caused by a change in flow velocity. The classic water hammer effect may be affected by transient cavitation, unsteady friction, fluid-structure interaction (FSI) and viscoelastic behaviour of the pipe wall [3]. Transient cavitating pipe flow occurs as a result of very low pressures during water hammer events. This paper deals with transient vaporous cavitation (column separation) that occurs when the pressure drops to the liquid vapour pressure. The amount of free and/or released gas in the liquid is assumed to be small. This is usually the case in most industrial pipeline systems. Two distinct types of transient vaporous cavitation may occur. The first type is a localized (discrete) vapour cavity with a large void fraction. A discrete vapour cavity may form at a boundary (valve, pump, turbine) or at a high point along the pipeline. In addition, an intermediate cavity may form as a result of the interaction of two low-pressure waves along the pipe. The second type of cavitation is distributed vaporous cavitation that may extend over long sections of the pipe. The void fraction for this case is small (close to zero). Distributed vaporous cavitation occurs when a rarefaction wave progressively drops the pressure in an extended region of the pipe to the liquid vapor pressure. The collapse of a vapour cavity may induce short-duration pressure pulses with values higher than the pressure initially given by the Joukowsky equation. Bergant and Simpson [4] classified column separation flow regimes regarding the physical state of the liquid and the maximum pipeline pressure as:

(i) **Active column separation flow regime.** The maximum pipeline pressure is generated following the column separation at the valve and along the pipeline (active column separation from the designer's perspective). The maximum pressure at the valve is governed by the intensity of the short duration pressure pulse.

(ii) **Passive column separation flow regime.** The maximum pipeline pressure is the water hammer pressure before intense cavitation occurs.

The value of the friction factor during unsteady flow is different than its value during steady flow. The friction factor can be expressed as a sum of two parts: 1) steady and 2) unsteady [5]. The unsteady part mimics transient-induced changes in flow conditions (velocity profile, turbulence intensity), and it is important for some unsteady flow situations. For pipelines that are not completely fixed, FSI effects have to be taken into account [6]. Viscoelastic pipe-wall behaviour is important in cases in which the pipe is made from plastic material such as high-density polyethylene [7]. Rapid filling and emptying of the pipeline may be considered to be a specific case in which both vaporous and gaseous cavities may be present [8]. Engineers should be able to predict all these events in piping systems and take appropriate measures to keep water hammer loads within the prescribed limits. There is a strong need for well-controlled

measurements of the water hammer effects; therefore, a flexible pipeline apparatus for investigating water hammer, transient cavitating flow, unsteady skin friction, fluid-structure interaction, and pipeline filling and emptying has been developed and installed at the University of Montenegro [9]. The small-scale apparatus consists of an upstream end high-pressurized tank, horizontal steel pipeline (total length 55.37 m, inner diameter 18 mm), four valve units positioned along the pipeline including the end points, and a downstream end tank (outflow tank). This paper investigates the effects of vaporous cavitation caused by the closure of the downstream end ball valve against the discharge. Comparisons between the results of two distinct water column separation tests and numerical simulations using an advanced discrete gas cavity model [10] are presented and discussed.

2 THEORETICAL MODELLING

Water hammer in liquid-filled pipelines is fully described by the continuity equation and equation of motion [1], [2],

$$\frac{\partial H}{\partial t} + \frac{a^2}{gA} \frac{\partial Q}{\partial x} = 0, \quad (2.1)$$

$$\frac{\partial H}{\partial x} + \frac{1}{gA} \frac{\partial Q}{\partial t} + \frac{fQ|Q|}{2gDA^2} = 0. \quad (2.2)$$

Note that all symbols are defined in the Nomenclature. Water hammer equations are valid only when the pressure is above the liquid vapour pressure. A quasi-steady approach for estimating skin friction losses (QSF) in the pipeline is satisfactory for slow transients only, [11]. Equations (2.1) and (2.2) are solved by the method of characteristics (MOC) using the staggered numerical grid, [1]. At a boundary (reservoir, valve, turbine), a device-specific equation is used instead of one of the MOC water hammer compatibility equations.

Some numerical models have been developed for simulation of transient vaporous cavitating pipe flow. One of them is a discrete gas cavity model (DGCM) that performs accurately over a broad range of input parameters [4]. The DGCM allows gas cavities to form at all computational sections within the MOC numerical grid. A liquid phase with a constant wave speed is assumed to occupy the computational reach. The DGCM is fully described by the two water hammer compatibility equations as a result of the MOC-transformation of Eqs. 2.1 and 2.2, and two additional equations; the continuity equation for the gas volume and the ideal gas equation with assumption of isothermal behaviour of the free gas, respectively, [1], [4],

$$\frac{d\forall_g}{dt} = Q_{out} - Q_{in}, \quad (2.3)$$

$$\forall_g = \alpha_0 \forall \left(\frac{P_0^*}{P_g^*} \right). \quad (2.4)$$

The numerical solution of DGCM equations can be found elsewhere, [1], [4].

Column separation is a relatively short duration event with a wide range of rapid flow event types. For rapid transients, the unsteady friction model is needed for the proper estimation of skin friction losses during transient events, [11]. The friction factor can be expressed as a sum of the quasi-steady part f_q and the unsteady part f_u , [5]

$$f = f_q + f_u. \quad (2.5)$$

The quasi-steady friction factor f_q depends on the Reynolds number and relative pipe roughness. A number of unsteady friction models have been proposed in the literature including one-dimensional (1D) and two-dimensional (2D) models. In this paper, an improved convolution based unsteady friction model [12] is used in DGCM, [10]. The convolution-based model (CBM) has been analytically developed by Zielke for transient laminar flow, [13]. This model produces correct results for some flow types using analytical expressions. The unsteady friction term f_u is defined as, [12]:

$$f_u = \frac{32\nu A}{DQ|Q|} \sum_{k=1}^N y_k(t). \quad (2.6)$$

The quantity y_k accounts for weights of past velocity changes. It is expressed as a recursive expression; theoretical derivation for y_k is given in, [12].

3 DESCRIPTION OF PIPELINE APPARATUS

A small-scale pipeline apparatus has been designed and constructed at the Faculty of Mechanical Engineering, the University of Montenegro, [9], for investigating water hammer, column separation, fluid-structure interaction, and pipeline filling and emptying. The apparatus is comprised of a horizontal pipeline that connects the upstream end high-pressurized tank and the outflow tank (steel pipe of total length $L = 55.37$ m; internal diameter $D = 18$ mm; pipe wall thickness $e = 2$ mm; maximum allowable pressure in the pipeline $p_{max, all} = 25$ MPa) – see Fig. 1. Four valve units are positioned along the pipeline including the end points. Valve units at the upstream end tank (position 0/3) and at the two equidistant positions along the pipeline (positions 1/3 and 2/3) are comprised of two hand-operated ball valves (valves $V_i/3U$ and $V_i/3D$; $i = 0, 1, 2$) that are connected to the intermediate pressure transducer block. Recently an additional T-section with two shut-off valves has been added to the upstream end valve unit (position 0/3) to facilitate pipeline filling and emptying tests, [14]. There are four 90° bends along the pipeline with radius $R = 3D$. The pipeline is anchored against the axial movement at 37 points (as close as possible to the valve units and bends). Loosening of the anchors is planned for fluid-structure interaction tests. The air pressure in the upstream end tank (total volume $\forall_{HPT} = 2$ m³; maximum allowable pressure in the tank $p_{HPTmax, all} = 2.2$ MPa) can be adjusted up to 800 kPa. The pressure in the tank is kept constant during each experimental run by using a high-precision air pressure regulator in the compressed air supply line, [9]. The upstream end tank is supplied with water from the tap water supply system. The operating air for the electro-pneumatically actuated ball valve (valve $V3/3P$) can be adjusted to between 200 to 400 kPa, yielding valve opening and closing times from 10 to 20 ms. The $V3/3P$ is operated by a solenoid valve (Bürkert 5/2) and a pneumatic actuator (Prisma). In addition, a hand-operated ball valve (valve $V3/3H$) is positioned next to the electro-pneumatically actuated ball valve.

valve angle during valve closing and opening events. Figure 2 shows the layout of the downstream end valve unit with instruments. The initial discharge (Q_0) and, consequently, the initial flow velocity (V_0) are measured with different methods ($U_x = \pm 1\%$). For initial flow velocities larger than 0.3 m/s, an electromagnetic flow meter Khrono OPTIFLUX 4000F IFC 300C is used. Smaller steady state velocities are estimated from the Joukowski pressure head rise or drop resulting from the rapid valve action. The water temperature is continuously monitored with the thermometer ($U_x = \pm 0.5^\circ \text{C}$) installed in the outflow tank. The water hammer wave speed was determined as $a = 1340 \text{ m/s}$ ($U_x = \pm 1\%$). Column separation experiments presented in this paper have shown a good repeatability of the magnitude and timing of the main pressure pulses.



Figure 2: Layout of downstream end valve unit with instruments.

4 COMPARISONS OF COMPUTED AND TEST RESULTS

This section presents numerical and experimental results from two distinct column separation runs including active and passive column separation cases [4]. Numerical results from the discrete gas cavity model with consideration of (1) quasi-steady friction (DGCM+QSF) and (2) unsteady skin friction (DGCM+CBM) [10] are compared with results of measurements performed in the laboratory pipeline apparatus – see Fig. 1. The two runs were carried out for a rapid closure of the hand-operated ball valve positioned at the downstream end of the horizontal pipe (valve V3/3H in Fig. 1). The sampling frequency for each dynamically measured quantity was $f_s = 2000 \text{ Hz}$. Pressures measured at the end points (positions 0/3 and 3/3) and at the two equidistant positions along the pipeline (positions 1/3 and 2/3) are compared with computational results as

piezometric heads (heads) with a datum level at the top of the horizontal pipe (elevation 0.0 m in Fig. 1). The number of reaches for all computational runs were $N = 108$.

4.1 Active column separation case

The active column separation case represents a transient event with a maximum head rise larger than the Joukowski head rise ($\Delta H_J = (a/g)V_0$), [4]. The initial flow velocity and the upstream end reservoir head were $V_0 = 0.44$ m/s and $H_{HPT} = 30.5$ m, respectively. Numerical and experimental results for this case are depicted in Figs. 3 and 4. The effective valve closure time of 0.025 s was much less than the wave reflection time $2L/a$ of 0.08 seconds. A rapid valve closure generates a column separation event with limited cavitation. The valve closure first induced Joukowski head rise at the valve ($\Delta H_J = 60$ m) and subsequently in time $t = 0.09$ s column separation at the valve. The negative wave travels along the pipeline and drops the head to the vapour pressure head at all measured positions along the pipeline. The maximum measured head at the valve $H_{3/3max} = 125$ m occurs as a short-duration pressure pulse after the first cavity collapses. The duration of the maximum measured head is very short (0.015 s).

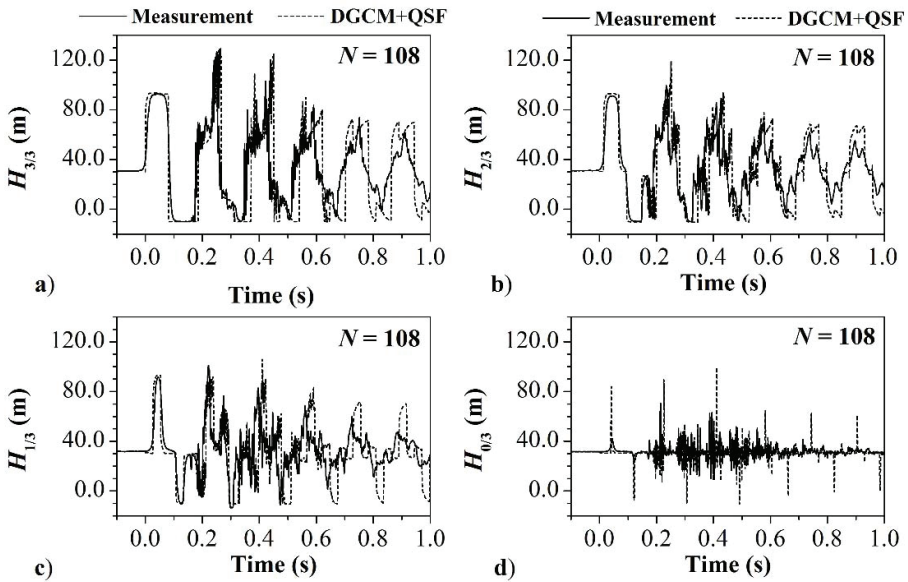


Figure 3: Comparisons of measured and DGCM+QSF-calculated heads at the end points ($H_{0/3}$ and $H_{3/3}$) and at the two equidistant positions along the pipeline ($H_{1/3}$ and $H_{2/3}$); $V_0 = 0.44$ m/s.

The maximum head obtained by DGCM+QSF (Fig. 3) is slightly higher than the measured one; it is $H_{3/3max} = 128$ m. In contrast, the maximum computed head predicted by DGCM+CBM (Fig. 4) is slightly lower $H_{3/3max} = 110$ m. The difference between the measured and calculated heads is due to the slightly different timing of the cavity collapse. The DGCM+QSF model gives good agreement with measured results for the first two pressure pulses. After that, a phase shift is obvious as well as lesser

attenuation of pressure traces (Fig. 3). This is not the case for DGCM+CBM results. The results agree well with the measured results during the whole period of observation (Fig. 4).

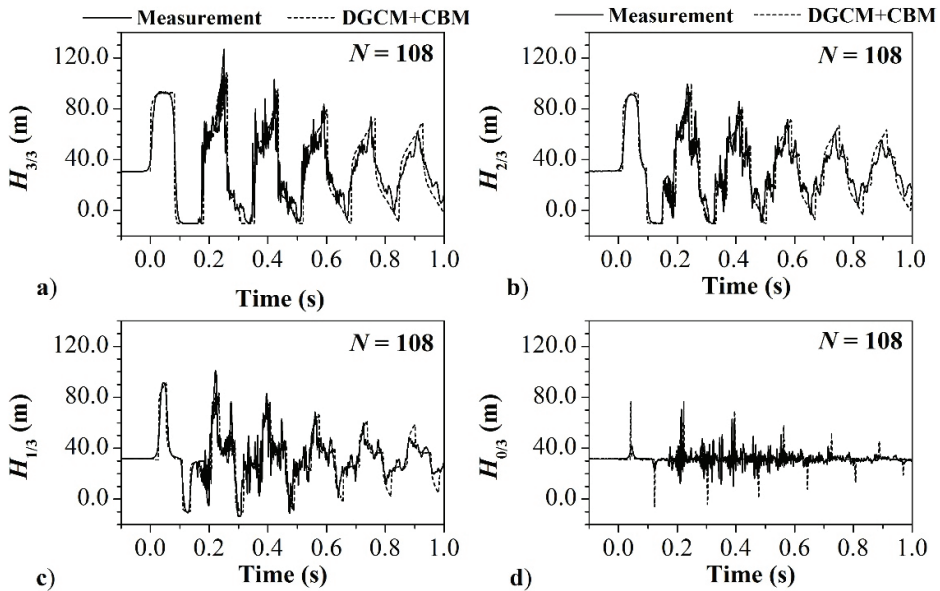


Figure 4: Comparisons of measured and DGCM+CBM-calculated heads at the end points ($H_{0/3}$ and $H_{3/3}$) and at the two equidistant positions along the pipeline ($H_{1/3}$ and $H_{2/3}$); $V_0 = 0.44$ m/s.

4.2 Passive column separation case

The passive column separation case is a transient event with a maximum head rise equal to the Joukowski head rise (ΔH_J), [4]. The initial flow velocity and the upstream end reservoir head were $V_0 = 2.19$ m/s and $H_{HPT} = 48$ m, respectively. Numerical and experimental results for this case are shown in Figs. 5 and 6. The effective valve closure time of 0.020 s was much less than the wave reflection time $2L/a$ of 0.08 seconds, and it was about 50% of the total closure time. A rapid valve closure generates a column separation event with severe cavitation. The valve closure first induced a Joukowski head rise at the valve ($\Delta H_J = 300$ m excluding friction effect and $\Delta H_J = 315$ m with friction) and subsequently, in time $t = 0.09$ s, severe column separation at the valve. The negative wave travels along the pipeline and drops the head to the vapour pressure head at all measured positions along the pipeline. The maximum measured head at the valve $H_{3/3max} = 295$ m after the first cavity collapsed is less than the Joukowski head $H_J = 340$ m. Pressure histories along the pipeline (Figs. 5b to 5c and 6b to 6c, respectively) enable accurate tracing of distributed vaporous cavitation zones and intermediate cavities. For this case the maximum measured head at the valve $H_{3/3max} = 340$ m occurs as the Joukowski water hammer head at the valve just before the first liquid column separation.

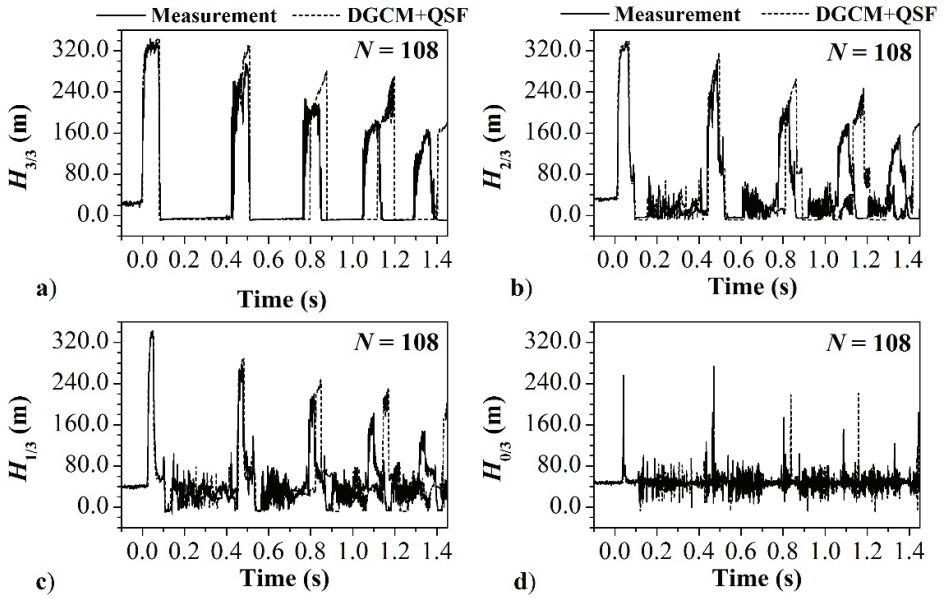


Figure 5: Comparisons of measured and DGCM+QSF-calculated heads at the end points ($H_{0/3}$ and $H_{3/3}$) and at the two equidistant positions along the pipeline ($H_{1/3}$ and $H_{2/3}$); $V_0 = 2.19$ m/s.

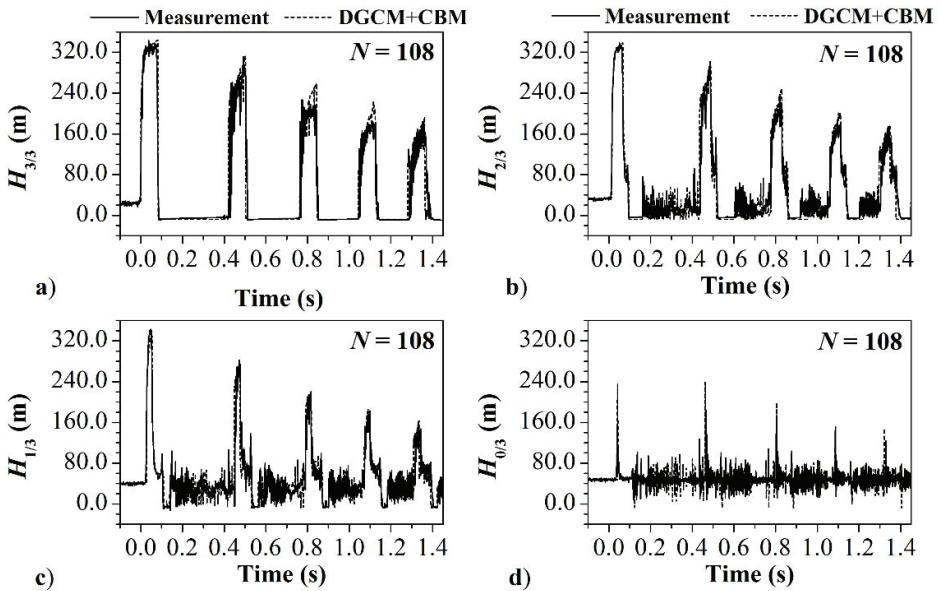


Figure 6: Comparisons of measured and DGCM+CBM-calculated heads at the end points ($H_{0/3}$ and $H_{3/3}$) and at the two equidistant positions along the pipeline ($H_{1/3}$ and $H_{2/3}$); $V_0 = 2.19$ m/s.

For the passive column separation case, the maximum measured and calculated pressure heads are in excellent agreement; see Figs. 5a and 6a, respectively. Again the DGCM+QSF model gives good agreement with the measured results for the first two bulk pressure pulses. After that, there are significant differences between the measured and calculated results (Fig. 5). In contrast, the DGCM+CBM results agree well with measured ones during the whole period of observation (Fig. 6).

5 CONCLUSIONS

Numerical results are compared with the results of the measurements given for the closure of the downstream end ball valve in the pipeline apparatus. Pressures measured at the end points (positions 0/3 and 3/3 in Fig. 1) and at the two equidistant positions along the pipeline (positions 1/3 and 2/3) are compared with computational results as piezometric heads (heads). Two distinct column separation runs include active and passive column separation cases. The DGCM model using a quasi-steady friction approach (DGCM+QSF) gives good agreement with the measured results for the first two pressure pulses. After that, there are significant differences between the measured and calculated results. In contrast, the advanced discrete gas cavity model with the consideration of unsteady skin friction (DGCM+CBM) performs well throughout the period of observation. Therefore, the discrete gas cavity model using the convolution-based unsteady friction term is recommended for engineering practice.

References

- [1] **E.B. Wylie, V.L. Streeter:** *Fluid Transients in Systems*, Prentice Hall, 1993
- [2] **M.H. Chaudhry:** *Applied Hydraulic Transients*, Springer, 2014
- [3] **A. Bergant, A.S. Tijsseling, J.P. Vítkovský, D.I.C. Covas, A.R. Simpson, M.F. Lambert:** *Parameters affecting water-hammer wave attenuation, shape and timing. Part 1: Mathematical tools and Part 2: Case studies*, Journal of Hydraulic Research, IAHR, Vol. 46, Iss. 3, Part 1, p.p. 373 – 381 and Part 2, p.p. 382 – 391, 2008
- [4] **A. Bergant, A.R. Simpson:** *Pipeline column separation flow regimes*, Journal of Hydraulic Engineering, ASCE, Vol. 125, Iss. 8, p.p. 835 – 848, 1999
- [5] **A. E. Vardy, J.M.B. Brown:** *Evaluation of unsteady wall shear stress by Zielke's method*, Journal of Hydraulic Engineering, ASCE, Vol. 136, Iss. 7, p.p. 453 – 456, 2010
- [6] **A. S. Tijsseling:** *Fluid-structure interaction in liquid-filled pipe systems: a review*, Journal of Fluids and Structures, Vol. 10, Iss. 2, p.p. 109 – 146, 1996
- [7] **D. Covas, I. Stoianov, F.J. Mano, H. Ramos, N. Graham, Č. Maksimović:** *The dynamic effect of pipe-wall viscoelasticity in hydraulic transients. Part I - experimental analysis and creep characterisation and Part II - model development, calibration and verification*, Journal of Hydraulic Research, IAHR, Part - I, Vol. 42, Iss. 5, p.p. 516 – 530 and Part - II, Vol. 43, Iss. 1, p.p. 56 – 70, 2004 and 2005

- [8] **A. Malekpour, W.B. Karney:** *Profile-induced column separation and rejoining during pipeline filling*, Journal of Hydraulic Engineering, ASCE, Vol. 140, Iss. 11, p.p. 04014054–1 – 12, 2014
- [9] **U. Karadžić, V. Bulatović, A. Bergant:** *Valve-induced water hammer and column separation in a pipeline apparatus*, Strojniški Vestnik – Journal of Mechanical Engineering, Vol.60, Iss. 11, p.p. 742 – 754, 2014
- [10] **A. Bergant, U. Karadžić, J.P. Vítkovský, I. Vušanović, A.R. Simpson:** *A discrete gas cavity model that considers the frictional effects of unsteady pipe flow*, Strojniški vestnik - Journal of Mechanical Engineering, Vol. 51, Iss. 11, p.p. 692 – 710, 2005
- [11] **A. Bergant, A.R. Simpson, J.P. Vítkovský:** *Developments in unsteady pipe flow friction modelling*, Journal of Hydraulic Research, IAHR, Vol. 39, Iss. 3, p.p. 249 – 257, 2001
- [12] **J. P. Vítkovský, M. Stephens, A. Bergant, M.F. Lambert, A.R. Simpson:** *Efficient and accurate calculations of Zielke and Vardy-Brown unsteady friction in pipe transients*, 9th International Conference on Pressure Surges, BHR Group, Chester, England, 2004
- [13] **W. Zielke:** *Frequency-dependent friction in transient pipe flow*, Journal of Basic Engineering, ASME, Vol. 90, Iss. 1, p.p. 109 – 115, 1968
- [14] **U. Karadžić, F. Strunjaš, A. Bergant, R. Mavrič, S. Buckstein:** *Developments in pipeline filling and emptying experimentation in a laboratory pipeline apparatus*, 6th IAHR Meeting of the Working Group Cavitation and Dynamic Problems in Hydraulic Machinery and Systems, Ljubljana, Slovenia, 2015

Nomenclature

(Symbols)	(Symbol meaning)
<i>A</i>	pipe area
<i>a</i>	water hammer wave speed
<i>D</i>	pipe diameter, diameter
<i>f</i>	friction factor
<i>f_s</i>	sampling frequency
<i>g</i>	gravitational acceleration
<i>H</i>	piezometric head, head
<i>L</i>	length
<i>N</i>	number of reaches; number of y_k components
<i>p</i>	pressure
<i>Q</i>	discharge
<i>t</i>	time
<i>U_x</i>	uncertainty in a measured quantity
<i>V</i>	flow velocity
<i>x</i>	distance along the pipe

y_k	component of the weighting function in Eq. 2.6
α	void fraction
ν	kinematic viscosity
ΔH	head rise
\forall	volume
(Subscripts)	(Subscripts meaning)
g	gas
HPT	high-pressurized tank, reservoir
in	inflow
J	Joukowsky head
max	maximum
out	outflow
q	quasi-steady part
u	unsteady part
0	initial conditions
(Superscripts)	(Superscripts meaning)
*	absolute pressure
(Abbreviations)	(Abbreviations meaning)
CBM	Convolution-Based Model
DGCM	Discrete Gas Cavity Model
FSI	Fluid-Structure Interaction
MOC	Method Of Characteristics
QSF	Quasi-Steady Friction

Acknowledgments

The authors wish to thank Slovenian Research Agency (ARRS) and Ministry of Science, Montenegro (MSM) for their support for this research conducted through the projects BI-ME/14-15-016 (ARRS, MSM) and L2-5491 (ARRS).